From Prototype to Flight: Qualifying a Ka-band Parabolic Deployable Antenna (KaPDA) for CubeSats

Jonathan Sauder[1], Nacer Chahat[2], Brian Hirsch[3], Richard Hodges[4], and Eva Peral[5]
Jet Propulsion Laboratory, California Institute of Technology. Pasadena, CA, 91109

Yahya Rahmat-Samii[6]
University of California Los Angeles. Los Angeles, CA, 90095

Mark W. Thomson[7]
Northrop Grumman Astro Aerospace. Carpinteria, CA, 93013

CubeSats have experienced a number of exciting technological advancements in the past several years. However, until recently, there has been very limited development in the area of high gain CubeSat antennas, which are critical for both high data rate communications and radar science. A Ka-band high gain antenna would provide a 10,000 times increase in data communication rates over an X-band patch antenna and a 100 times increase over state-of-the-art S-band parabolic antennas. Because of this, three years ago the Jet Propulsion Laboratory (JPL) initiated a research and technology development effort to advance CubeSat communication capabilities, with one of the key thrusts being the Ka-band parabolic deployable antenna (KaPDA). This antenna started with the ambitious goal of fitting a 42 dB, 0.5 meter, 35 Ghz antenna in a 1.5U canister. This paper discusses the process of taking the antenna from a first prototype to the flight design, how the design successfully met its goals, and lessons learned. A prototype antenna was constructed in early 2015, and then upgraded to an engineering model at the end of 2016. KaPDA will be flying on the RainCube mission, and earth science CubeSat. KaPDA is the second deployable parabolic antenna to fly on a CubeSat, and the first of its kind to operate at Ka-band enabling a number of opportunities for high rate deep space antenna communications and radar science.

I. Introduction

CubeSats have recently seen a large increase in technical capabilties and launch opportunties, including potential missions beyond low earth orbit. As instruments become more advanced and operational distances between CubeSats and earth increases, data rates become a mission limiting factor. Improving CubeSat data rates has become critical enough for NASA to establish the CubeQuest Centennial Challenge[1] where one of the key metrics is transmitting as much data as possible from the moon and beyond. Currently, many CubeSats communicate on UHF bands, with those that are viewed as having high data rate abilities using S-band or X-band patch antennas. The CubeSat ANEAS, which was launched in September 2012, pushed the envelope with a half-meter S-band dish which could achieve 100x

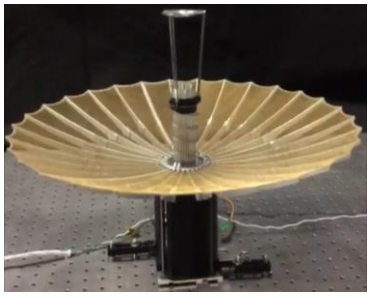

Figure 1. KaPDA

[1] Mechatronics Engineer, Technology Infusion, 299-101, 4800 Oak Grove Drive, Pasadena, CA, AIAA Member
[2] RF Engineer, Spacecraft Antennas, 161-260, 4800 Oak Grove Drive, Pasadena, CA
[3] Mechatronics Engineer, Deployable Structures, 299-101, 4800 Oak Grove Drive, Pasadena, CA, AIAA Member
[4] Technical Group Supervisor, Spacecraft Antennas, 161-260, 4800 Oak Grove Drive, Pasadena, CA
[5] Technical Group Supervisor, Digital Radar Electronics, 161-260, 4800 Oak Grove Drive, Pasadena, CA
[6] Professor, Electrical Engineering, 6731K Boelter, 420 Westwood Plaza, Los Angeles, CA
[7] Chief Engineer, 6384 Via Real, Carpinteria, CA, AIAA Fellow

© 2016. All rights reserved. Government sponsorship acknowledged.

the data rate of patch antennas. A half-meter parabolic antenna operating at Ka-band would increase data rates by over 100x that of the ANEAS antenna and 10,000x that of X-band patch antennas. Further, various radar missions are enable by large aperture high frequency parabolic antennas. This would be particularly useful for Earth monitoring CubeSat constellations.

II. Background

A number of deployable parabolic and parabolic like antennas have been developed in the past for CubeSats. Concepts have included a goer-wrap composite reflector[2], a reflector transformed from the CubeSat body[3], an inflatable parabolic reflector with reflecting material on one side and transparent material on the other[4], a mesh reflector supported by ribs[5,6], and a reflectarray[7]. While these designs provide unique solutions, they are all designed to operate at S-band (with the exception of the reflectarray, which is also currently under development at the Jet Propulsion Laboratory). A Ka-band antenna would have much greater gain, which translates to greater data rate, but requires a much higher surface accuracy than an S-band antenna. The lack of high gain antennas motivated JPL to launch a research and development effort for high frequency deployable antennas for CubeSats three years ago.

Deployable antenna concepts can be organized by architecture, each of which have strengths and weaknesses in meeting CubeSat communication needs. Architectures include solid deploying reflectors, shape memory reflectors, inflatables, reflectarrays, and mesh reflectors. Solid deploying reflectors have great surface accuracy, but do not stow well in small spaces and can be heavy (e.g. Hughes spring-back antenna[8]). Shape memory reflectors may work at lower frequencies, but much development is still required as at Ka-band the surface is not accurate enough[9]. Inflatable reflectors stow well and are lightweight but have issues with maintaining inflation and shape. This is especially problematic on interplanetary CubeSat missions which will likely last much longer than LEO CubeSat missions. Reflectarray antennas provide a relatively high gain and stow well in large flat spaces (i.e. areas for solar panels on a CubeSat), but have very limited operational frequency range, thus requiring two separate antennas, one to transmit and the other to receive. Therefore, the most attractive high gain deployable antenna design for JPL to pursue was the mesh reflector architecture.

There are many concepts for mesh parabolic deployable antennas at much larger scales than CubeSats. In the 1970's Lockheed Martin developed the Wrap-Rib reflector, which uses a mechanism to wrap the ribs and mesh like a tape measure[10]. However, the design does not fit well in the CubeSat form factor, as the mechanism that deploys and stows the ribs is quite large. There are also a number of knit mesh reflectors, the most popular of which are Harris's Unfurlable Antenna and Northrop Grumman's AstroMesh[9]. However, these two designs consist of many small, detailed components, which are challenging to scale down without the antenna becoming prohibitively expensive. It should be noted that about two years after the start of JPL's initiative, others began developing CubeSat antenna designs inspired by the AstroMesh and Unfurlable Antenna configurations, but both have larger apertures and are likely to consume more volume than the antenna discussed in this paper[11,12].

At the point the Ka-band antenna effort began three years ago, two knit mesh antennas had been developed for CubeSats, but both were designed for S-band operation. They were a spiral stowed rib design[6] and the ANEAS parabolic deployable antenna (APDA) folding rib design that was used on USC/ISI's ANEAS spacecraft[5]. The spiral stowed rib design, while very compact, would be challenging to extend to Ka-band as the ribs could not apply adequate force required to stretch Ka-band mesh to achieve the required surface accuracy. The APDA architecture would work well for Ka-band, as it used straight folding ribs, which can apply more force and allow for greater surface accuracy. In addition, the APDA is the only CubeSat parabolic deployable antenna to have flown. Therefore, it was decided to use the APDA as a starting point for the Ka-band parabolic deployable antenna (KaPDA) design[13,14].

III. Design of the Mechanical Prototype

The first design task was to analyze the influence of antenna configurations on stowed space and gain. A number of designs were explored including Cassegrainian, Gregorian, and several hat-style feeds[15]. The Cassegrainian configuration was selected as it best balanced performance and stowed size, as the dimensions for the sub-reflector were such that it could be stowed within 1.5U.

The number of ribs supporting the mesh structure is a key factor for achieving surface accuracy, which is critical at Ka-Band. More ribs result in a more ideal dish, and thus greater RF gain. However, as the number of ribs increase, the clearance between each rib when stowed decreases. Packing ribs too tightly could result in snagging during deployment. The best compromise between rib clearance and RF loss due to a non-ideal shape was found to be 30 ribs.

© 2016. All rights reserved. Government sponsorship acknowledged.

Each rib was divided into two components, the root rib and tip rib, which were connected by the mid rib hinge. The mesh forces and resulting moments determined the geometry of the rib. As the root ribs experienced the greatest bending moment, they were deeper. The tip rib had a tapered design to conserve space and eliminate material where it was not required for rigidity. The taper was designed to create an even stress profile throughout the rib. To improve both stowing efficiency and surface accuracy, the ribs were much deeper (by over 10 times) but slightly thinner than those used on APDA. The deep rib design also was advantageous for precisely controlling the rib's deployed position.

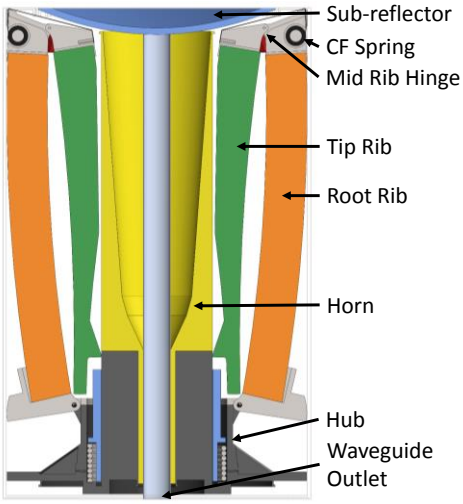

Figure 2. Key KaPDA Components

Perhaps the greatest design challenge was developing a deployment mechanism that stowed in 1.5U with the antenna. The deployment mechanism must first push the hub out of the CubeSat and then unfold the ribs. The APDA was deployed entirely using springs, with all the components unfolding quickly. However, Ka-band requires 40 opening per inch (OPI) mesh which is stiffer and required greater deployment forces than 10 OPI mesh APDA used. A preload of approximately 250N was required at the end of the spring's displacement, which means any stowed spring would likely be compressed to well over 500 N resulting in a violent deployment. Therefore, other concepts for deploying the hub and ribs had to be explored.

To deploy the hub, a number of concepts were explored including a motor driving a threaded rod, a scissors lift, low force springs (if hub deployment was decoupled from rib deployment), cables and pulleys driven by motors, and a gas driven piston. Many concepts were eliminated because of complexity (e.g. cables and pulleys driven by motors), they were challenging to implement within the highly constrained space (e.g. scissors lift), or they didn't work (e.g. low force springs). Initially, the most attractive deployment mechanism was the gas driven piston, as it stowed well in a small space. To actuate the antenna, two micro CGG's, built by CGG technologies, would provide enough gas to deploy the antenna to the required pressure in the vacuum of space [16]. After deployment, a latch was used to lock the hub in place to ensure if the gas escaped the antenna would remain fully deployed.

To deploy, the hub was first driven upwards by compressed gas pushing on a piston (Figure 3, A-B). As the hub neared the top of the canister, the root rib base hinges caught on a snap ring and the ribs began to deploy (B-C). The tip ribs reached a point where they became free of the horn interference, and the constant force springs deployed them (Image C). The hub continued to travel upwards until the root ribs fully deployed (image D). As the ribs folded outwards, the sub-reflector was released by the root rib hinges and telescoped along the horn, pushed upward and held in place by a spring (C to D). After the hub was fully deployed, it was locked into place by spring-loaded latches.

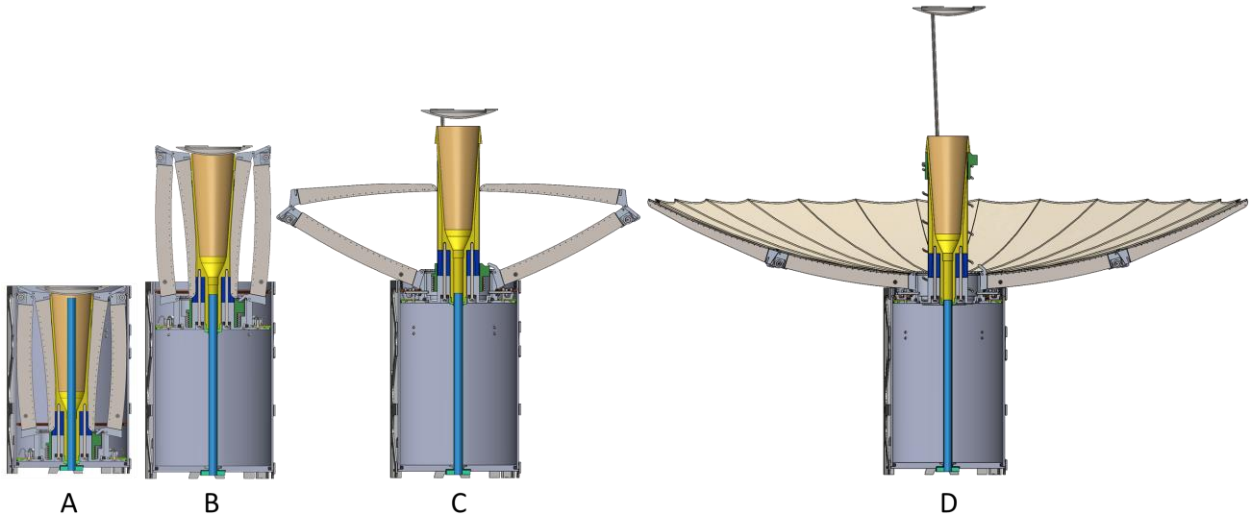

Figure 3. KaPDA Deployment Sequence

© 2016. All rights reserved. Government sponsorship acknowledged.

IV. Antenna Modifications from Prototype

The mechanical prototype was tested for deployment using an air supply and adjustable valve. While deployment initially appeared successful, when the antenna was taken to the RF range for testing, it was found some of the ribs were not latched in the deployed state. Detailed investigation into the slow motion videos of the deployment revealed that during deployment the antenna hub tilted to one side, as it neared the top of the canister, only straightening itself after the ribs began to deploy. This tilt prevented some of the ribs from latching into place on the hub. After manually latching the hub, the antenna assumed its shape and it was possible to RF test the antenna. However, there was a degradation in RF performance (Table 1) and manual adjustment is not possible on orbit, therefore it was necessary to explore other deployment solutions.

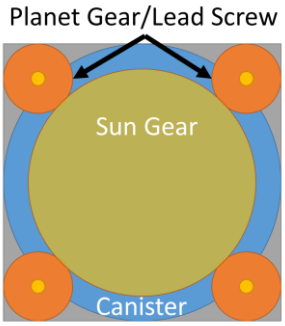

Figure 4. Four Lead Screws Provide a Level, Controlled Deployment

The primary problem with the air powered design was that nothing kept the hub axially aligned with the waveguide near the end of deployment. While the waveguide preliminarily kept the hub aligned, as it neared the top of the canister in Figure 3C, there was not adequate length over diameter to ensure the two stayed axial until full deployment. Unlike springs or other actuator concepts, air does not provide any stabilization or centering capabilities. Further investigations into the CGG's also revealed actuation occurred quite suddenly, on the order of 10ths of a second, which would result in a deployment with comparative violence to that of springs. Therefore, another deployment approach was required.

About this time, serendipitously a small 10 mm motor with a 1024:1 gearbox was found. Investigation revealed the motor and gearbox combination could produce the required torque when applied through a lead screw. A properly designed lead screw would also keep the hub aligned axially with the waveguide. A key design challenge with this architecture was connecting the lead screw to the hub, as the most intuitive design would place it at the center of the antenna. However, the telescoping Ka-band waveguide was located at the center of the antenna, and there was no room to place a lead screw without interfering with the RF design, which is why this design was not considered earlier.

A solution was found by utilizing four lead screws instead of one, located in the four unused corners of the canister (Figure 4). The four lead screws kept the hub axial to the waveguide at all times. However, to ensure a smooth deployment, all four lead screws had to deploy synchronously. To maintain synchronization, the four lead screws were attached to "planet" gears which mated with one "sun" gear. A single motor drove one of the planet gears, which was then transferred to the other planet gears through the "sun" gear. The deployment sequence occurred in the same fashion as illustrated in Figure 3, except now the hub was moved upwards in the canister by the lead screws instead of by expanding gas.

The motorized design provided a number of other advantages, beyond a controlled deployment and keeping the hub axially aligned with the waveguide. It also eliminated the need for all latches and a launchlock, as preload from the lead screws were used to secure the antenna in the stowed position and retain it in the fully deployed position. Given the low pitch of the lead screws, it is virtually impossible for launch or deployment loads to back drive the screws, thus providing a secure latch. Using a motorized deployment provides a controllable deployment sequence, as a motor controller governs motor rate and position of the antenna and the encoder provides feedback on the number of shaft revolutions, providing deployment status. Further utilizing a motor decreases deployment test cost,

Measure	Units	Goal	Simulation	Pre-Deploy	Gas Deploy	Motor Deploy
Stowed Size	U (10x10x11.3cm^3)	1.5	1.36	1.36	1.36	1.43
Deployed Diameter	m	0.5	0.51	0.51	0.51	0.51
Gain	dB	42	42.6	42.5	42.0	42.6
Beam Width	degrees	1.2	1.2	1.2	1.2	1.2
RMS Surface Accuracy	mm	0.40	N/A	0.22	0.25	--
Mass	Kg	3.0	1.9	1.2	1.2	1.2
Thermal	°C	-17 to 35	--	-25 to 85	--	-0 to 85

Table 1: Comparison of KaPDA Performance

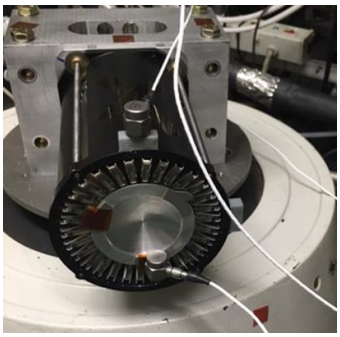

Figure 5. KaPDA Engineering Model on Vibration Shaker in Y-axis orientation

© 2016. All rights reserved. Government sponsorship acknowledged.

as each CGG costs several thousand dollars, and eliminates the risk of a high pressurized can of gas which could potentially spin up the CubeSat if any leaks occurred.

The canister and base of the hub were replaced on the existing prototype to enable the addition of the gear train and motor, upgrading the prototype to an engineering model. The antenna was then deployment tested a second time, and produced better RF results than the prototype version. It was calculated that the motorized deployment provides more preload than the latches, which results in a more robust antenna shape. This likely created the 0.5 dB increase in gain indicated in Table 1 between the gas and motorized deployments. This meant the motorized antenna performed just as well after deployment, as the antenna performed in the original pre-deployed position.

V. Antenna Qualification Testing

After the motorized deployment mechanism was successful demonstrated, the upgraded engineering model antenna was stowed and subjected to a series of vibration tests, simulating launch loads. The goal was to qualify the antenna to GEV's protoflight levels[17], at 14.1 G_{rms} in three axes. To determine the antenna response, accelerometers were mounted on both the antenna canister and the sub-reflector (Figure 5). The test began with a 0.5 G sine sweep to 10 to 2000 Hz, to identify the antenna's response at different frequencies. Then, a vibration tests was performed at 1.77 G_{rms}, followed by another sine sweep. This pattern continued for 5 G_{rms} and 7 G_{rms} vibration tests with careful inspection of the antenna after each vibration to ensure nothing was broken. After each test, the pre and post 0.5 G sine sweeps were also compared, to see if there was any significant change to the antennas response across frequencies. A change in response indicates a change in the structure of the antenna, which means a bolted joint could have slipped or a part could have been structurally damaged. After the 7 G_{rms} test in the Y-axis, significant changes in the sine sweep were observed (Figure 7 left). Several dynamics experts were consulted for advice, and it was determined because the antenna contained a number of "loose" ribs, as the mid-rib hinges were free to rotate slightly, the variations in sine sweep response were not a good indicator of a loss of structural integrity. A simple shift in the position of the hinged components could lead a different response. The dynamicists suggested a better indicator instead of the sine sweep would be to perform a low level random vibration test, at 1.77 G_{rms} before and after the each test. Because the stochastic nature of the random vibration test, it should average out the differences in hinge position at a specific frequency, and thus be a better indicator of structural integrity. A 10 G_{rms} vibration test was performed with a 1.77 G_{rms} test preceding and following the test. As indicated in Figure 6 right, the responses from the pre and post 1.77 G_{rms} random vibration test were very similar.

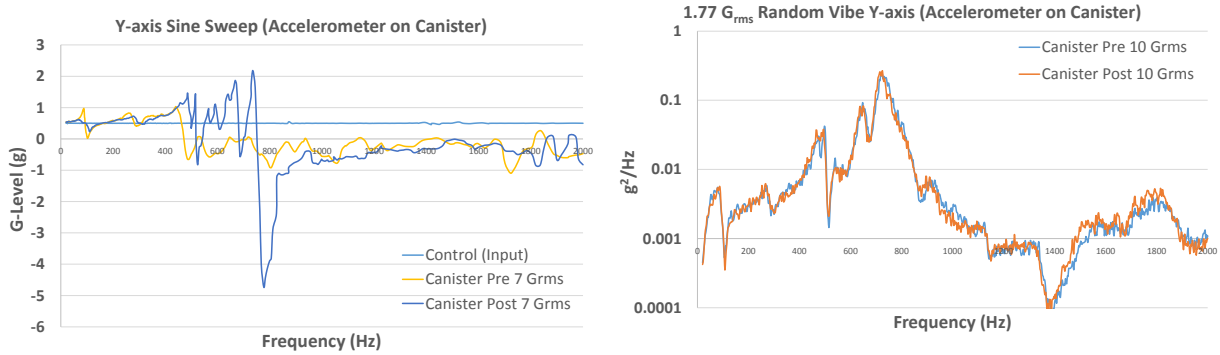

Figure 6. Sine Wave Sweep (left) and Random Vibe (right) Response

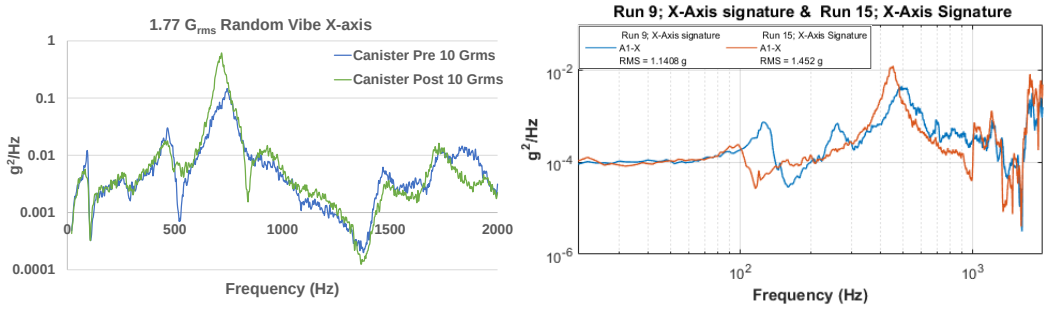

Figure 7. Random Vibration of the Antenna (left) and CubeSat P-POD (right)

© 2016. All rights reserved. Government sponsorship acknowledged.

When switching the antenna from the Y-axis to the X-axis, and performing a 10 G_{rms} vibration test, the results from the pre and post 1.77 G_{rms} response seemed to indicate a structural shift (Figure 7 left). While the difference was not as significant as the pre and post sine sweep tests, the results had a change in response at 500 Hz, 700 Hz, and 1700 Hz. The antenna was removed from the fixture, and inspected for damage, but none could be found in the stowed condition. To ensure there was no damage before proceeding with the more intense 14.1 G_{rms} test, it was deemed necessary to deploy the antenna.

Figure 8. Partially Deployed Antenna

The antenna was deployed for a third time, and while no damage was found, another problem was observed. The mid-rib hinges, actuated by the constant force spring did not deploy (Figure 8, contrast to Figure 1). This was an unexpected result, as this phenomenon had never before been observed. It was known that the mid rib hinges had a low torque margin, but prior deployments had never failed to deploy the antenna. A number of tests were run on an extra single rib, and the root cause was eventually found to be friction. When the antenna was stowed, as the constant force spring is unrolled and pulled across the root portion of the mid-hinge, it has a little bit of extra tension generated by friction (Figure 9 top). However, during vibration, the spring relaxed to its lowest energy state, and the friction that was originally giving the spring slightly more tension aiding deployment, was now working against deployment (Figure 9 center). The combination of deploying against gravity and the springs being held by friction in a more relaxed state resulted in a negative torque margin. To remedy this issue, small spring steel kick-off diving boards were added, which gave the spring a slightly longer moment arm, allowing it to deploy (Figure 9 bottom). This small modification nearly doubled the torque.

After deployment, the antenna appeared to be in the same condition as it was prior to vibration, with no indications of damage. The small deviation in the mid rib constant force spring could not solely explain the difference in the random vibration test (Figure 8 left). If the structure was not completely fixed inside the antenna canister, could this lead to variations in in the random vibration response, and did it not average out as was originally expected? To answer this question, additional sources of data were examined. A similar situation to loose ribs in a canister occurs with a CubeSat inside a generic P-POD deployer, where the CubeSat is free to vibrate by a few millimeters within the volume. Accelerometer data from the exterior of a P-POD deployer from another JPL project was obtained for comparison (Figure 7 right). While sometimes the pre and post random vibration data aligned, similar to Figure 6 right, many other times the data was found to be markedly different (Figure 7 right). Therefore, it was determined for structures that have some degree of freedom, and are not fixed, it is normal for both the pre and post sine sweeps and the random vibration tests to not align. It should be noted the pre and post random vibration produced a more consistent response than the pre and post sign sweep.

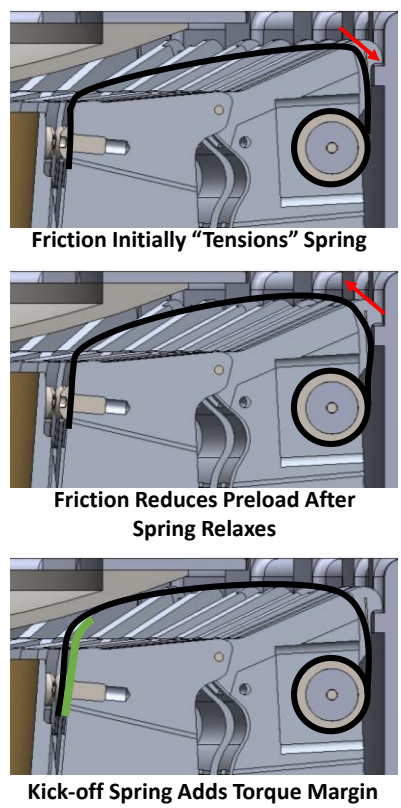

Figure 9. Mid Rib Hinge

After the antenna was altered to place kick-off springs on a number of hinges and it was determined the variations in response of the random vibration curves were to be expected, it was deemed safe to continue the test campaign with a 14.1 G_{rms} vibration test in all three axis, which proceeded without incident. The engineering model antenna was successfully deployed after the vibration test, and was taken to the RF range to analyze performance. It was found there was no change in performance before or after the vibration test, with a measured gain of 42.7 dBi (the measurement accuracy is approximately ± 0.2 dBi). Nearly as impressive as the post vibration performance, is that the antenna has been deployed over a half-dozen times, and has consistently held the same performance.

Successful demonstration of KaPDA after vibration meant construction could begin on the flight Ka-band Radar Parabolic Deployable Antenna (KaRPDA) for RainCube, a precipitation Ka-band Radar mission. RainCube is a technology demonstration mission, which is anticipated to be the first active radar in a CubeSat. The KaRPDA mid rib hinge geometry was modified to provide a greater moment arm, such that the kick-off springs used on the engineering model were not required. Construction of the flight antenna was completed in October, and the finished antenna began environmental testing in November. Thus far, the antenna has been

© 2016. All rights reserved. Government sponsorship acknowledged.

successfully deployed in thermal vacuum, with the deployment mechanisms being demonstrated at both 0°C and 55°C. Next the flight antenna will undergo vibration testing, but given the success of past tests on the engineering model, similar results are expected.

VI. Conclusion

The Ka-band Parabolic Deployable Antenna (KaPDA) has demonstrated its ability to exceed its goals through testing the prototype, engineering model, and flight antenna. The antenna is lower mass, fits in a smaller volume, provides higher gain, and is a larger diameter than initially anticipated. The antenna has successfully performed through environmental testing, although some small modifications have been required. Several key takeaways from this endeavor, which can generally be applied to deployables are:

1) Be cautious when utilizing single use deployment mechanisms, especially ones that cannot be easily controlled, liked the original inflation concept for KaPDA.
2) Expect that pre and post vibration response patterns for non-fixed structures will vary.
3) Consider the effects of friction in deployment mechanisms, especially when a component relaxes to its lowest energy state through vibration.

KaPDA will create opportunities for a host of new CubeSat missions by allowing high data rate communication and high fidelity radar instruments, such as its first opportunity to fly on RainCube. It is scheduled for a launch in March of 2018. It is thrilling to think about the number of new opportunities KaPDA opens up.

Acknowledgments

The research was carried out at the Jet Propulsion Laboratory, California Institute of Technology, under a contract with the National Aeronautics and Space Administration. Authors thank Leah Ginsberg, David Hunter, Ted Steiner, and Savannah Velasco student interns, for their work on the mechanical design, Michael Johnson, Michelle Easter, Josh Ravich, and Kim Aaron who provided advice on the design, Brian Merrill (Spectrum Marine and Model Services), Hugo Rodriguez, Pedro Moreira, Natalie Lockwood-Barajas, Gerry Gaughen, Building 103 Techs and Rudy Herrera who assisted in building the antenna, and Dr. Jefferson Harrell who performed the RF tests.

References

[1] Mohon, L., "NASA's Cubequest Challenge," *NASA* Available: http://www.nasa.gov/directorates/spacetech/centennial_challenges/cubequest/index.html.

[2] Reynolds, W., Murphey, T., and Banik, J., "Highly Compact Wrapped-Gore Deployable Reflector," *52nd AIAA/ASME/ASCE/AHS/ASC Structures, Structural Dynamics and Materials Conference*, American Institute of Aeronautics and Astronautics, .

[3] Shirvante, V., Johnson, S., Cason, K., Patankar, K., and Fitz-Coy, N., "Configuration of 3U CubeSat Structures for Gain Improvement of S-band Antennas," *AIAA/USU Conference on Small Satellites*, Aug. 2012.

[4] Babuscia, A., Corbin, B., Knapp, M., Jensen-Clem, R., Van de Loo, M., and Seager, S., "Inflatable antenna for cubesats: Motivation for development and antenna design," *Acta Astronautica*, vol. 91, Oct. 2013, pp. 322–332.

[5] Aherne, M., Barrett, T., Hoag, L., Teegarden, E., and Ramadas, R., "Aeneas -- Colony I Meets Three-Axis Pointing," *AIAA/USU Conference on Small Satellites*, Aug. 2011.

[6] MacGillivray, C. "Scott," "Miniature High Gain Antenna for CubeSats," Apr. 2011.

[7] Hodges, R., Shah, B., Muthulingham, D., and Freeman, T., "ISARA – Integrated Solar Array and Reflectarray Mission Overview," *AIAA/USU Conference on Small Satellites*, Aug. 2013.

[8] Tan, L. T., and Pellegrino, S., "Stiffening Method for 'Spring-Back' Reflectors," Athens, Greece: ISASR, 2000.

[9] Bassily, S., and Thomson, M., "Deployable Reflectors," *Handbook of Reflector Antennas and Feed Systems Volume 3: Applications of Reflectors*, Boston, Massachusetts: Artech House, 2013.

[10] Davis, G., and Tanimoto, R., "Mechanical Development of Antenna Systems," *Spaceborne Antennas for Planetary Exploration*, John Wiley & Sons, 2006.

[11] "SMALL SATELLITE ANTENNAS: 1-Meter Unfurlable Mesh Antenna," *Harris Government Communciations Systems* Available: http://govcomm.harris.com/#1-meter unfurlable mesh antenna.

[12] "ROC-Rib Deployable Ka-Band Antenna for Nanosatellites | SBIR.gov" Available: https://www.sbir.gov/sbirsearch/detail/1149555.

[13] Sauder, J., Chahat, N., Hodges, R., Thomson, M., Rahmat-Samii, Y., and Peral, E., "Designing, Building, and Testing a Mesh Ka-band Parabolic Deployable Antenna (KaPDA) for CubeSats," *54th AIAA Aerospace Sciences Meeting*, San Diego: AIAA, 2016.

[14] Sauder, J., Chahat, N., Hodges, R., Thomson, M., and Rahmat-Samii, Y., "Ka-band Parabolic Deployable Antenna (KaPDA) Enabling High Speed Data Communication for CubeSats," *AIAA SPACE 2015 Conference and Exposition*, Pasadena, CA: AIAA, 2015.

© 2016. All rights reserved. Government sponsorship acknowledged.

[15] Chahat, N., Hodges, R., Sauder, J., Thomson, M., Peral, E., and Rahmat-Samii, Y., "CubeSat deployable Ka-band mesh reflector antenna development for Earth science missions," *IEEE Transactions on Antennas and Propagation*, vol. PP, 2016, pp. 1–1.
[16] "Micro CGG" Available: http://cgg-technologies.com/wp-content/uploads/2013/07/Flyer-Space-Micro-CGG-2013-2.pdf.
[17] Milne, J. S., and Kaufman, D. S., *General Environmental Verification Specification*, 2003.

© 2016. All rights reserved. Government sponsorship acknowledged.